Invited Paper

Simulations of directed energy comet deflection

Qicheng Zhang*[a], Philip M. Lubin[a], Gary B. Hughes[b]

[a]Dept. of Physics, Univ. of California, Santa Barbara, CA, USA;
[b]Statistics Dept., California Polytechnic State Univ., San Luis Obispo, CA, USA

Abstract

Earth-crossing asteroids and comets pose a long-term hazard to life and property on Earth. Schemes to mitigate the impact threat have been studied extensively but tend to focus on asteroid diversion while neglecting the possibility of a comet threat. Such schemes often demand physically intercepting the target by spacecraft, a task feasible only for targets identified decades in advance in a restricted range of orbits. A threatening comet is unlikely to satisfy these criteria and so necessitates a fundamentally different approach for diversion. Comets are naturally perturbed from purely gravitational trajectories through solar heating of their surfaces which activates sublimation-driven jets. Artificial heating of a comet, such as by a high-powered laser array in Earth orbit, may supplement natural heating by the Sun to purposefully manipulate its path to avoid an impact. The effectiveness of any particular laser array for a given comet depends on the comet's heating response which varies dramatically depending on factors including nucleus size, orbit and dynamical history. These factors are incorporated into a numerical orbital model using established models of nongravitational perturbations to evaluate the effectiveness and feasibility of using high-powered laser arrays in Earth orbit or on the ground to deflect a variety of comets. Simulation results suggest that orbital arrays of 500 m and 10 GW operating for 10 min/d over 1 yr may be adequate for mitigating impacts by comets up to ~ 500 m in diameter. A 100 m diffraction-limited ground-based array at 10 GW may be similarly effective when appropriately located.

Keywords: comets, high-powered lasers, planetary defense

1. INTRODUCTION

Near-Earth Objects (NEOs), including both asteroids and comets, pose a long-term hazard to human interests on Earth. Many schemes to mitigate the impact threat have been developed but generally focus on the asteroid threat with minimal attention toward cometary impactors. Such schemes include, but are not limited to

- kinetic impactors, by which momentum is transferred to the asteroid via the hypervelocity impact of an expendable spacecraft, optionally enhanced by an explosive charge[1,2]
- direct application of thrust, via thrusters placed directly onto the surface of the asteroid[3] or on a large "gravity tractor" spacecraft positioned nearby[4]
- surface albedo alteration, such as by paint[5] or mirrors[6] to slowly shift the asteroid's orbit via radiation pressure

These strategies share the fundamental requirement that a spacecraft must physically intercept the target. This requirement is acceptable when the target follows a typical low-eccentricity, low-inclination orbit and is identified decades in advance of a potential impact. While such a condition holds for many near-Earth asteroids (NEAs) and even some Jupiter-family comets (JFCs), others, like Halley-type comets (HTCs) and long-period comets (LPCs) follow high-eccentricity, high-inclination orbits and are often discovered within 2 yr of their perihelia, and thus, their encounters with Earth.[7] Such a short timescale limits the availability of maneuvers like gravity assists, necessitating an impractically large delta-v for any interception mission.

Orbital diversion through laser ablation avoids the fundamental interception restriction.[8] In this strategy, a laser array concentrates energy onto the surface of the target, vaporizing it. The resulting ejecta plume exerts

* corresponding author — email: qicheng@cometary.org

Planetary Defense and Space Environment Applications, edited by Gary B. Hughes, Proc. of SPIE
Vol. 9981, 998108 · © 2016 SPIE · CCC code: 0277-786X/16/$18 · doi: 10.1117/12.2235711

thrust on the object, shifting it from its original collisional trajectory. The effectiveness of asteroid deflection has been analyzed for several mission configurations.[9] One option suitable for deflecting NEAs is, in fact, to have the laser intercept and travel alongside the asteroid. Physical proximity of the laser, however, is not a fundamental necessity for the directed energy approach. The long-range nature of light implies that a laser array may also be built to operate from Earth orbit or even from the ground, deflecting the target remotely. Such a system would permit an immediate response to any confirmed threat, including HTCs and LPCs.

2. SIMULATIONS

Simulations model the Sun, the Moon and the eight known major planets as Newtonian gravitational point sources in the frame of the solar system barycenter with their positions given by JPL DE 421.[10] The comet is treated as a test particle under the influence of the gravitational sources and of the laser which is approximated as coincident with the center of the Earth at position $\boldsymbol{x}_\oplus$. Numerical integration is performed with the "s17odr8a" composition of the Velocity Verlet method.[11]

2.1 Laser

Comet deflection performed by heating of the target comet by a large array of phased laser elements. Two classes of laser arrays are considered:

1. Orbital: the laser array is supported by a photovoltaic (PV) array operating in low-Earth orbit. Laser output is restricted by both an operating power P, constrained by the number of laser elements and by their heat dissipation mechanisms, and a time-averaged power $\langle P \rangle$, constrained by the size and efficiency of the PV array. In the simulations, the laser operates at P when active supported both by the PV array directly and by an attached battery system charged by the PV array when the laser is idle.

2. Ground: the laser array is installed directly on the Earth's surface. Laser output is restricted to P primarily by the size of the array and the number of laser elements available. Electrical power and heat dissipation capacity impose lesser constraints. Mean power $\langle P \rangle = f(t)P$ varies over time t, where $f(t)$ is the average fraction of time each day the laser can target the comet. For the laser to be usable, the comet must be within the laser's field of view of diameter Θ_{fov} centered on the zenith, a condition dependent on the latitude of the laser ϕ_{las} and on the declination of the comet $\delta_{\text{com}}(t)$ as viewed from Earth. Furthermore, $f(t) \propto \kappa$, the fraction of acceptable the weather expected at the site of the laser. Although κ may vary on a seasonal basis depending on local climate, these variations are neglected for the simulations in which κ is considered constant. Careful treatment of κ is left to a more detailed study on laser site selection.

Both arrays are assumed to be capable of producing a diffraction-limited beam diverging at a half-angle $\theta_{\text{beam}} \approx \lambda_{\text{beam}}/L_{\text{las}}$ for a beam of wavelength $\lambda_{\text{beam}} \approx 1\,\mu$m from a laser of characteristic size L_{las}. In the case of the ground array, an adaptive optics system is necessary to attain such a narrow beam. Such challenges faced in the construction of these arrays have been, and are continuing to be analyzed in detail separately and will not be discussed in depth here.[8] Unless otherwise noted, the simulations assume these purely engineering challenges may be overcome.

2.2 Comet

The target comet is modeled as a non-rotating spherical comet with a semi-empirical nongravitational acceleration model[12] fitted to a numerically-computed sublimation curve of water ice snow on the comet's surface.[13] Such a comet at position $\boldsymbol{x}$ illuminated by the Sun at $\boldsymbol{x}_\odot$, with $r \equiv \|\boldsymbol{x} - \boldsymbol{x}_\odot\|$, experiences a nongravitational acceleration, produced by jets powered by sublimating ices, of

$$\ddot{\boldsymbol{x}}_{\text{NG}} = A \times 0.111262(r/r_0)^{-2.15}(1 + (r/r_0)^{5.093})^{-4.6142}(\boldsymbol{x} - \boldsymbol{x}_\odot)/r \tag{1}$$

where $r_0 = 2.808\,$au. The nongravitational parameter A (the acceleration at $r = 1\,$au) varies by several orders of magnitude between different comets depending on dynamical age, structure and size.[14] Assuming thrust $F_{\text{NG}} = m_{\text{com}}\ddot{x}_{\text{NG}}$ is proportional to the area of the cross section of sunlight intercepted by the comet, the

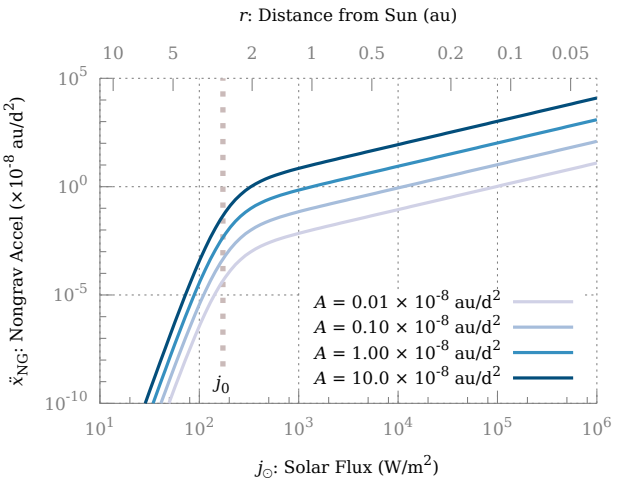

Figure 1. The nongravitational acceleration of a comet varies as a function of incident flux, and thus distance to the Sun, as given by Equation 1 and Equation 2. The nongravitational parameter A spans a possible range of several orders of magnitude between different comets depending on surface composition (related to age) and size of which a selection of possible values are plotted.[14] Two different regimes are evident: Below a critical flux $j_0 = 172.6\,\mathrm{W/m^2}$ (corresponding to $r_0 = 2.808\,\mathrm{au}$), acceleration falls off rapidly as $\ddot{x}_{\mathrm{NG}} \propto j^{12.83}$. Above j_0, the function becomes nearly linear, approaching $\ddot{x}_{\mathrm{NG}} \propto j^{1.075}$.

nongravitational parameter is $A \propto R_{\mathrm{com}}^{-1} \implies A \equiv A_{1\,\mathrm{km}}\,(1\,\mathrm{km}/2R_{\mathrm{com}})$ for comets of similar dynamical age and origin of diameter $2R_{\mathrm{com}}$.

The simulations assume that energy absorption by the comet is wavelength-neutral. Then, the comet must necessarily respond to all incident radiation equivalently regardless of its origin, with the response depending only on the flux j on the comet. By this equivalence principle, *any* radiation source at $\boldsymbol{x}_0$ (with $r' \equiv \|\boldsymbol{x} - \boldsymbol{x}_0\|$) uniformly illuminating the cross section of the comet—including a laser with a beam that has sufficient diverged to a cross section larger than the comet—will produce an acceleration

$$\ddot{\boldsymbol{x}}_{\mathrm{NG}} = A \times 0.111262(j/j_0)^{1.075}(1 + (j/j_0)^{-2.5465})^{-4.6142}(\boldsymbol{x} - \boldsymbol{x}_0)/r' \tag{2}$$

where $j_0 = 172.6\,\mathrm{W/m^2}$ is the solar flux at $r = r_0$, given a total solar irradiance of $S_0 = 1361\,\mathrm{W/m^2}$ at $r = 1\,\mathrm{au}$.[15] The magnitude of single-source nongravitational acceleration is plotted in Figure 1 in the context of the Sun.

Equation 2, however, only gives the acceleration from a single radiation source and is valid, for example, when the comet is only being illuminated by the Sun, or is only being illuminated by the laser. In comet deflection scenario, both sources must generally be considered. As Equation 2 is highly nonlinear, the acceleration from the superposition of the two-sources is nontrivial and necessitates additional assumptions on the actual distribution of thrust on the comet's surface.

Consider two radiation sources 1 and 2, representing the Sun and the laser, illuminating the comet separated by angle θ as illustrated in Figure 2. The illuminated fraction of the comet is divided into three regions:

1. region A: illuminated by source 1 alone
2. region B: illuminated by source 2 alone
3. region C: illuminated by both

Due to the curvature of the comet's surface, the surface itself is not uniformly-illuminated in any of the three regions despite the cross section being uniformly-illuminated. Precise determination of the acceleration contributed by each region requires a detailed thermal model for the surface response to incident radiation. Results

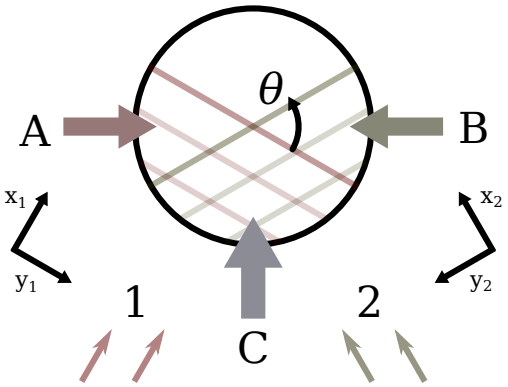

Figure 2. A comet being deflected is, in general, illuminated from two different directions by two different radiation sources (the Sun and the laser). In this diagram, source 1 illuminates the lower left (red stripes) of the comet (circle) and source 2 illuminates the lower right (green stripes), with the sources separated by an angle θ. The illuminated fraction of the comet is divided into three regions: region A illuminated by source 1 alone, region B illuminated by source 2 alone, and region C illuminated by both. Arrows directed into the comet indicate the assumed direction of acceleration contributed by each region—the mean inward normal direction of the region—used in the simulations.

from such a model only be accurate for a perfectly spherical comet and remains a rough approximation for the acceleration of a realistic comet. Comparable accuracy to a realistic comet may therefore be attained by simply considering the acceleration contributed to by each region to be the mean inward normal direction of the region as indicating in Figure 2.

Choose $\hat{\boldsymbol{x}}_1$ to be the propagation direction of radiation from source 1 and $\hat{\boldsymbol{y}}_1$ a perpendicular direction in the plane of both sources and the comet as indicated in Figure 2. When source 2 is inactive (ie. no laser), the two-source model—the sum of the accelerations contributed by region A and region C—must be consistent the single source model. Let $\ddot{\boldsymbol{x}}_A$ be the acceleration contributed by region A and $\ddot{\boldsymbol{x}}_C$ be the acceleration by region C. The sum $\ddot{\boldsymbol{x}}_1 \equiv \ddot{\boldsymbol{x}}_A + \ddot{\boldsymbol{x}}_C$ must match the expression for $\ddot{\boldsymbol{x}}_{\mathrm{NG}}$ given in Equation 2. Matching the components in $\hat{\boldsymbol{x}}_1$ and $\hat{\boldsymbol{y}}_1$ gives

$$\begin{cases} \ddot{x}_1 &= \ddot{x}_A \sin(\theta/2) + \ddot{x}_C \cos(\theta/2) \\ 0 &= \ddot{x}_A \cos(\theta/2) - \ddot{x}_C \sin(\theta/2) \end{cases} \tag{3}$$

so $\ddot{x}_A = \ddot{x}_1 \sin(\theta/2)$ and $\ddot{x}_C = \ddot{x}_1 \cos(\theta/2)$ are the magnitudes of the acceleration contributions of the two regions.

When source 2 is activated, region A experiences no change, so $\ddot{x}_A$ remains unaffected. By symmetry, region B contributes an acceleration of $\ddot{x}_B = \ddot{x}_2 \sin(\theta/2)$, where $\ddot{\boldsymbol{x}}_2$ is the acceleration given by Equation 2 for source 2 alone. Finally, the acceleration contributed by region C becomes roughly $\ddot{x}_C = \ddot{x}_{1+2} \cos(\theta/2)$ where $\ddot{\boldsymbol{x}}_{1+2}$ is the acceleration by Equation 2 for a single source with the combined flux of both source 1 and source 2. The net nongravitational acceleration on the comet is then the vector sum

$$\ddot{\boldsymbol{x}}_{\mathrm{NG}} = \ddot{\boldsymbol{x}}_A + \ddot{\boldsymbol{x}}_B + \ddot{\boldsymbol{x}}_C \tag{4}$$

This two-source model degenerates into special cases of the one-source model as expected in both the $\theta \to 0$ limit (ie. comet at distance $r \gg 1\,\mathrm{au}$, the separation of the Sun and the Earth/laser), where $\ddot{\boldsymbol{x}}_{\mathrm{NG}} \to \ddot{\boldsymbol{x}}_{1+2}$, and in the $\theta \to \pi$ limit (ie. comet directly between Sun and laser) where $\ddot{\boldsymbol{x}}_{\mathrm{NG}} \to \ddot{\boldsymbol{x}}_1 + \ddot{\boldsymbol{x}}_2$, a simple superposition of the one-source accelerations.

In the simulations, source 1 is the Sun with an incident flux $j_1 = S_0 \times (1\,\mathrm{au}/r)^2$. Source 2 is the laser, at distance $\Delta \equiv \|\boldsymbol{x} - \boldsymbol{x}_\oplus\|$ from the comet, produces a spot of radius $R_{\mathrm{spot}} = \theta_{\mathrm{beam}}\Delta$ with flux $j_2 = P_{\mathrm{peak}}/\left(\pi R_{\mathrm{spot}}^2\right)$ when active.

The two-source model above is only valid when $R_{\mathrm{spot}} > R_{\mathrm{com}}$, a condition needed for the cross section of the comet to be uniformly illuminated. In the limit $j_2 \gg j_1$ and $R_{\mathrm{spot}} \ll R_{\mathrm{com}}$ (but with R_{spot} still sufficiently large to neglect thermal diffusion, a condition assumed to always hold), the laser-contributed acceleration decouples from the solar acceleration $\ddot{\boldsymbol{x}}_\odot$ in Equation 1 to give

$$\ddot{\boldsymbol{x}}_{\mathrm{spot}\ll\mathrm{com}} = \ddot{\boldsymbol{x}}_\odot + \left(R_{\mathrm{spot}}/R_{\mathrm{com}}\right)^2 \ddot{\boldsymbol{x}}_2 \tag{5}$$

where $\ddot{\boldsymbol{x}}_2$ is the one-source acceleration by a laser of the same flux j_2 illuminating the entire comet cross section.

For intermediate $R_{\mathrm{spot}} < R_{\mathrm{com}}$ but $R_{\mathrm{spot}} \not\ll R_{\mathrm{com}}$, linear interpolation (in area) between the $R_{\mathrm{spot}} \to 0$ limit and the case $R_{\mathrm{spot}} \to R_{\mathrm{com}}$ with $j_2 \to j_2' = j_2\left(R_{\mathrm{spot}}/R_{\mathrm{com}}\right)^2$ is used. Total nongravitational acceleration by the Sun and laser is therefore

$$\ddot{\boldsymbol{x}}_{\odot+\mathrm{las}} = \begin{cases} \left(1 - \left(R_{\mathrm{spot}}/R_{\mathrm{com}}\right)^2\right)\ddot{\boldsymbol{x}}_{\mathrm{spot}\ll\mathrm{com}} + \left(R_{\mathrm{spot}}/R_{\mathrm{com}}\right)^2 \ddot{\boldsymbol{x}}_{\mathrm{NG}}(j_1, j_2') & \text{if } R_{\mathrm{spot}} < R_{\mathrm{com}} \\ \ddot{\boldsymbol{x}}_{\mathrm{NG}}(j_1, j_2) & \text{if } R_{\mathrm{spot}} \geq R_{\mathrm{com}} \end{cases} \tag{6}$$

When $\langle P \rangle < P$, the laser is idle for a fraction of time and $\ddot{\boldsymbol{x}}_{\mathrm{NG}}$ becomes an appropriate linear combination of $\ddot{\boldsymbol{x}}_{\odot\ \mathrm{only}}$ from Equation 1 with the Sun alone, and $\ddot{\boldsymbol{x}}_{\odot+\mathrm{las}}$ from Equation 6 with the Sun and laser together:

$$\ddot{\boldsymbol{x}}_{\mathrm{NG}} = \left(1 - \langle P\rangle/P\right)\ddot{\boldsymbol{x}}_{\odot\ \mathrm{only}} + \left(\langle P\rangle/P\right)\ddot{\boldsymbol{x}}_{\odot+\mathrm{las}} \tag{7}$$

Finally, it may not advantageous to keep the laser active, even when line of sight and power restrictions permit as perturbations to the orbit from laser heating at one part of the orbit may cancel perturbations from laser heating at a different part of the orbit.[9] Perturbation cancellation may be minimized by tracking the sign of $\xi \equiv (\boldsymbol{x}_{\mathrm{com}} - \boldsymbol{x}_\oplus) \cdot \dot{\boldsymbol{x}}_{\mathrm{com}}$ and permitting the laser to activate either only when $\xi > 0$ (laser is "behind") or only when $\xi < 0$ (laser is "ahead"). The simulations focus primarily on deflecting HTCs and LPCs which generally have long orbital periods $\gtrsim 50\,\mathrm{yr}$ with deflection occurring only over the final fraction of an orbit before its Earth encounter. Thus, $\xi < 0$ nearly always holds, so the laser "ahead" condition is chosen.

2.3 Numerical Setup

The original orbit of the comet is specified by its perihelion distance q, inclination i, eccentricity e, time of impact T, whether impact occurs at the ascending or descending node, and whether impact occurs when the comet is inbound or outbound.

Then, initial conditions for the comet are found by the following procedure:

1. Choose $\boldsymbol{x}_0(T) = \boldsymbol{x}_\oplus(T)$ as the final position of the comet in its natural orbit.
2. Compute $\dot{\boldsymbol{x}}_0(T)$ such that the heliocentric Keplerian orbit fit through $\boldsymbol{x}_0(T)$, $\dot{\boldsymbol{x}}_0(T)$ matches the specified orbital parameters.
3. Using the Keplerian orbit of the comet, find the smallest $\delta t > 0$ such that $\|\boldsymbol{x}_0(T - \delta t) - \boldsymbol{x}_\oplus(T - \delta t)\| = R_\oplus$, the radius of the Earth.
4. Increase $\dot{x}_0(T - \delta t) \to \dot{x}_0(T - \delta t) + \sqrt{2GM_\oplus/R_\oplus}$ to account for Earth's gravitational well.
5. Numerically integrate time-reversed system in the solar system potential with $\ddot{\boldsymbol{x}}_{\mathrm{NG}}$ from Equation 1 to find $\boldsymbol{x}(t_0)$, $\dot{\boldsymbol{x}}(t_0)$, the state vector at time $t = t_0$ when the laser is to be first activated.

Using $\boldsymbol{x}(t_0)$, $\dot{\boldsymbol{x}}(t_0)$ as initial conditions, numerical integration proceeds the same solar system potential with $\ddot{\boldsymbol{x}}_{\mathrm{NG}}$ from Equation 7. The system is integrated either to $t = T$ (yielding $\boldsymbol{x}(T)$, $\dot{\boldsymbol{x}}(T)$) or until $\Delta(t) \equiv \|\boldsymbol{x}(t) - \boldsymbol{x}_\oplus(t)\| < \mathrm{R}_\oplus$ where the comet impacts the Earth.

3. RESULTS

For each comet deflection scenario, a *deflection distance* $\Delta_{\rm def}$ quantifies the effectiveness of the deflection. For comets with a local minimum $\Delta_{\rm min} = \Delta(t_{\rm min}) > \mathrm{R}_\oplus$ (no impact), use $\Delta_{\rm def} = \Delta_{\rm min}$. Otherwise, define true time of impact $t_{\rm imp}$ by $\Delta(t_{\rm imp}) = \mathrm{R}_\oplus$ and $\dot\Delta(t_{\rm imp}) < 0$. Deflection distance $\Delta_{\rm def}$ is then defined as the corresponding $\Delta_{\rm min}$ for the trajectory $\boldsymbol{x}_1(t)$ with $\boldsymbol{x}_1(t_{\rm imp}) = \boldsymbol{x}(t_{\rm imp})$ and $\dot{\boldsymbol{x}}_1(t) = \dot{\boldsymbol{x}}(t_{\rm imp})$, the linear continuation of the comet's trajectory through the Earth.

In October 2014, a dynamically new comet, C/2013 A1 (Siding Spring), passed Mars at a distance $\sim 0.001\,$au just 22 months after its discovery.[16] An Earth-bound comet might follow a similar timeline with impact confirmation and laser activation at 1 yr prior to the Earth encounter. For the simulations, consider a similar $2R_{\rm com} = 500\,$m diameter comet with $A = 2 \times 10^{-8}\,\mathrm{au/d^2}$ ($A_{1\,\rm km} = 1 \times 10^{-8}\,\mathrm{au/d^2}$) in a comparable orbit of $q = 0.9\,$au, $e = 1$, $i = 130^\circ$ leading to an Earth impact at $T =$ J2000.0 at its ascending node while the comet is inbound. These parameters for this *canonical comet* are used for all simulations except when otherwise noted.

3.1 Orbital Laser

A laser array in Earth orbit is restricted in $\langle P\rangle$ by the size and efficiency of its PV array. Consider a square PV array with edge length $L_{\rm las}$, equal in size to the laser array. For a total solar-to-laser power efficiency $\varepsilon = 20\%$, such a system produces $\langle P\rangle = \varepsilon S_0 L_{\rm las}^2$. With ε constrained by technology and thermodynamics, $\langle P\rangle$ can only be improved by scaling up the array. Use of a supplementary battery system, however, allows $P \gg \langle P\rangle$.

Figure 3 illustrates the effectiveness of arrays with a range of $L_{\rm las}$, $\langle P\rangle$ and P for deflecting the canonical comet. Increasing array size $L_{\rm las}$ and efficiency ε both yield a substantial improvement in deflection distance $\Delta_{\rm def}$. Furthermore, even an increase in P alone leads to a significant increase in $\Delta_{\rm def}$, particularly at low P where the marginal increase in $\Delta_{\rm def}$ for P is comparable to the marginal increase for $\langle P\rangle$. This phenomenon is explained by the nonlinear behavior of Equation 1 illustrated in Figure 1. In the regime $j \ll j_0$, corresponding to when the comet is at a large distance Δ from the laser, $\ddot x_{\rm NG} \propto j^{12.83}$ where small increases in P are amplified into much larger increases in $\ddot x_{\rm NG}$ and thus $\Delta_{\rm def}$ by the large power of j. However, for sufficiently high P, the comet will be in the near-linear $j \gg j_0$ regime for the entirety of the deflection, and further increases in P will have little effect on $\Delta_{\rm def}$.

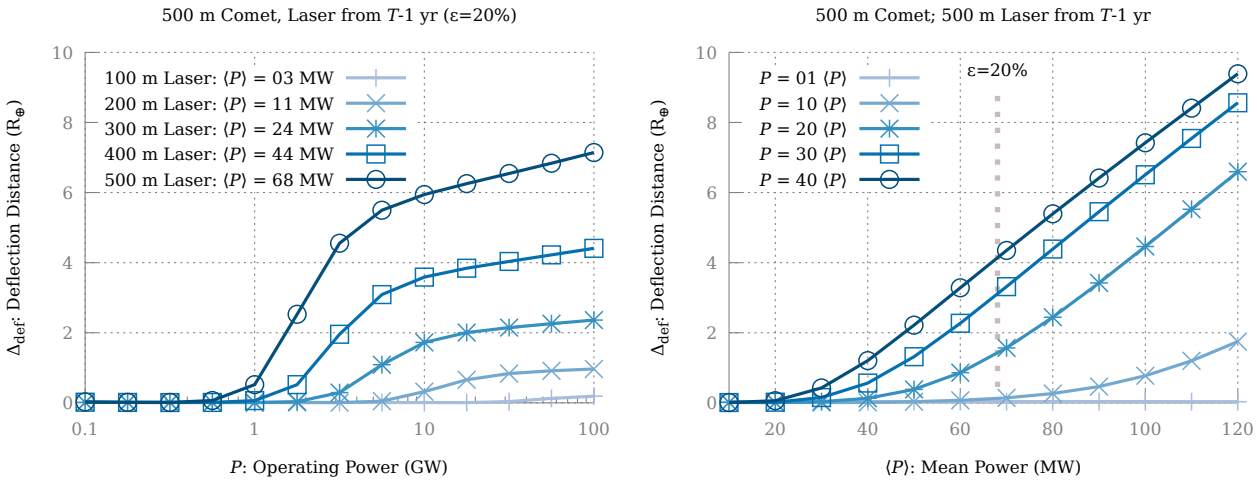

Figure 3. Orbital laser deflection of the canonical comet beginning 1 yr before its Earth encounter. Increasing P, even while leaving $\langle P\rangle$ unchanged (left), yields a substantial improvement in deflection at low P due to the comet being in the highly nonlinear $j \ll j_0$ regime in Figure 1. There is little further improvement once P is sufficiently high for the near-linear $j \gg j_0$ regime to dominate throughout the deflection period. With $P = 40\langle P\rangle = 2.7\,$GW (at $\varepsilon = 20\%$), the comet is deflected by $\Delta_{\rm def} = 4\,\mathrm{R}_\oplus$, compared to a negligible deflection under the same $\langle P\rangle$ but with $P = \langle P\rangle$ (right).

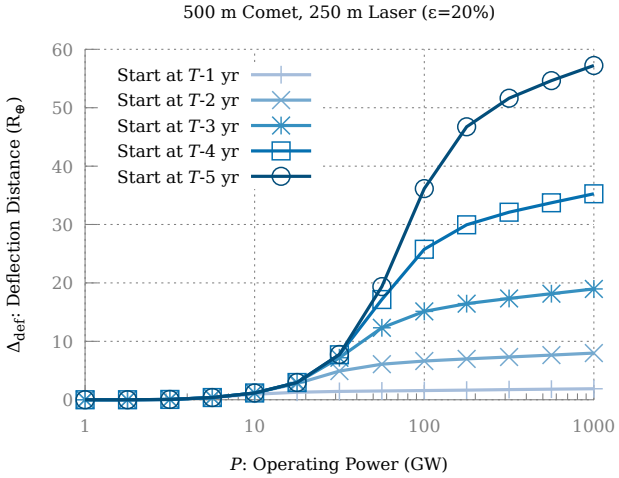

Figure 4. Starting deflection earlier is only of measurable benefit when using a sufficiently powerful laser producing sufficient flux on the comet to give non-negligible acceleration at the beginning of the deflection period. With a $L_{\rm las} = 250\,{\rm m}$ laser at $\varepsilon = 20\%$ efficiency, the laser must operate at $P \gtrsim 10\,{\rm GW}$ to justify starting earlier than $T - 1\,{\rm yr}$ and $P \gtrsim 30\,{\rm GW}$ for starting earlier than $T - 4\,{\rm yr}$. At $P = 1000\langle P\rangle = 17\,{\rm GW}$, the canonical comet is deflected $\Delta_{\rm def} = 6\,{\rm R}_\oplus$ when deflection begins at $T - 3\,{\rm yr}$ or earlier.

To deflect the canonical comet by a safe $\Delta_{\rm def} = 4\,{\rm R}_\oplus$, a $L_{\rm las} = 500\,{\rm m}$ laser must operate at $P = 2.7\,{\rm GW}$ ($P = 40\langle P\rangle$), or a $L_{\rm las} = 400\,{\rm m}$ laser at $P = 32\,{\rm GW}$ ($P = 730\langle P\rangle$). In contrast, neither array produces any measurable deflection if operating at a continuous $P = \langle P\rangle$.

It is conceivable that comet detection capability advances sufficiently by the time a threatening comet is identified that deflection may begin as early as $t_0 = T - 5\,{\rm yr}$ for larger comets which may permit the use of a smaller laser array. However, at such an early time, the comet is a large distance $r, \Delta \sim 15\,{\rm au}$ from both the Sun and the laser. Without a sufficiently high operating power, the flux on the comet will fall deep within the $j \ll j_0$ regime and little deflection will occur until the comet approaches to a much closer distance.

Figure 4 compares the effectiveness of several deflection start times for a smaller $L_{\rm las} = 250\,{\rm m}$ laser with $\varepsilon = 20\%$ efficiency. Below $P = 10\,{\rm GW}$, little benefit is gained in beginning deflection earlier than $T - 1\,{\rm yr}$. Operating at $P = 1000\langle P\rangle = 17\,{\rm GW}$, the canonical comet is deflected $\Delta_{\rm def} = 6\,{\rm R}_\oplus$ when deflection begins at $T - 3\,{\rm yr}$ or earlier.

Note that a laser at $P/\langle P\rangle = 1000$ would operate for an average of only 86.4 s each day during which the energy collected over an entire day is drained. Achieving such high $P/\langle P\rangle$ while maintaining ε may not necessarily be less of an engineering challenge than constructing a larger and equally effective array at lower $P/\langle P\rangle$. Analysis of optimal $P/\langle P\rangle$ is left to a more thorough investigation of orbital laser array construction. The remainder of this section considers arrays operating at a lower $P/\langle P\rangle = 100$.

Larger arrays are necessary to divert comets of $2R_{\rm com} \gtrsim 1\,{\rm km}$. Figure 5 shows that $\Delta_{\rm def} \propto R_{\rm com}^{-3}$ for a fixed $A_{1\,{\rm km}}$. Given 5 yr, a $L_{\rm las} = 500\,{\rm m}$ laser is sufficient to deflect a $2R_{\rm com} = 1\,{\rm km}$ comet by $\Delta_{\rm def} = 3\,{\rm R}_\oplus$. A larger $L_{\rm las} = 2\,{\rm km}$ laser can deflect the same comet by $\Delta_{\rm def} = 520\,{\rm R}_\oplus$ or a $2R_{\rm com} = 5\,{\rm km}$ by $\Delta_{\rm def} = 3\,{\rm R}_\oplus$. Large comets of $2R_{\rm com} \gtrsim 10\,{\rm km}$ require arrays of $L_{\rm las} \gtrsim 4\,{\rm km}$ to deflect. Impacts by such comets, however, are thought to be extremely rare, even on geologic timescales, averaging just one impact every 0.1 Gyr.[17]

Deflection effectiveness drops rapidly with decreasing array size. At $P/\langle P\rangle = 1000$, $L_{\rm las} = 250\,{\rm m}$ appears to be the smallest useful array for comet deflection and is capable of deflecting a small $2R_{\rm com} = 50\,{\rm m}$ comet by $\Delta_{\rm def} = 10\,{\rm R}_\oplus$. For even smaller comets, the damage potential is unlikely to be sufficient to justify the expense of deflection. Note that because the simulations assume A and $R_{\rm com}$ remain static throughout the deflection, results for small comets, which are more strongly altered by the deflection process, should be treated with caution.

Finally, because the solar system is not isotropic or even approximately isotropic about the Earth gravitationally, the deflection effectiveness of a given laser system varies depending on the exact orbit of the comet.

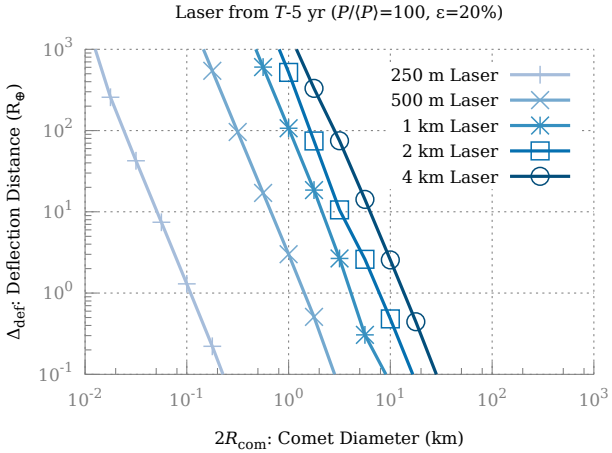

Figure 5. Deflection distance scales as $\Delta_{\rm def} \propto R_{\rm com}^{-3}$ for a fixed $A_{1\,\rm km}$. Operating at $P = 100\langle P\rangle$, $\varepsilon = 20\%$ for 5 yr, a $L_{\rm las} = 500\,$m laser is sufficient to deflect a $2R_{\rm com} = 1\,$km comet by $\Delta_{\rm def} = 3\,\mathrm{R}_\oplus$. A larger $L_{\rm las} = 2\,$km laser can deflect the same comet by $\Delta_{\rm def} = 520\,\mathrm{R}_\oplus$ or a $2R_{\rm com} = 5\,$km by $\Delta_{\rm def} = 3\,\mathrm{R}_\oplus$. Laser arrays of $L_{\rm las} \lesssim 250\,$m may not be economically viable for comet deflection due to the small size of comets that such arrays are capable of deflecting.

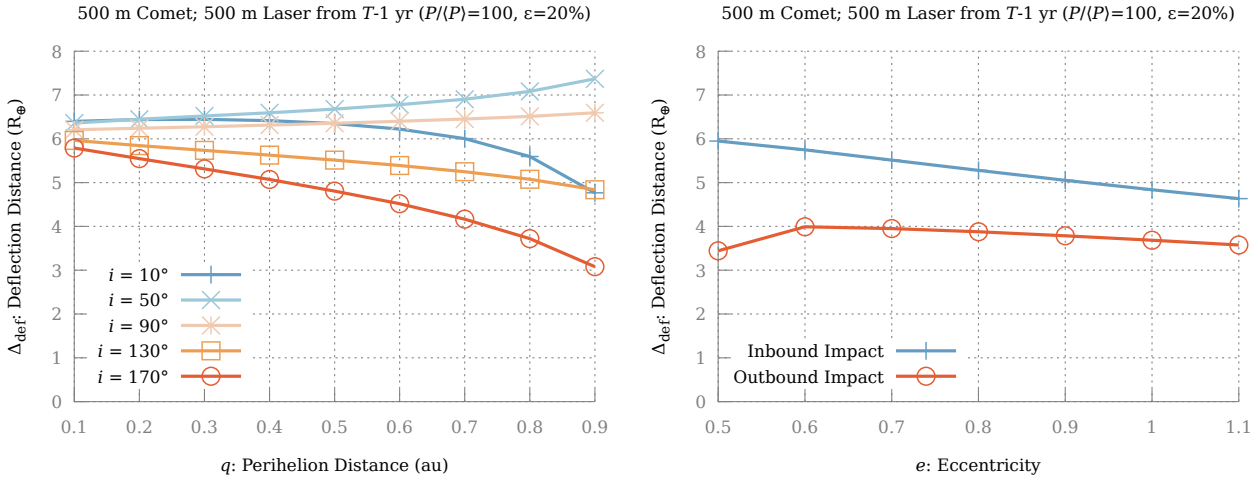

Figure 6. Deflection effectiveness varies up to a factor of 2 depending on the actual orbit of the comet. Deflection is most effective for orbits that place the comet near the laser for long durations over the deflection period. For deflection with a $L_{\rm las} = 500\,$m, $P = 100\langle P\rangle$ laser over 1 yr, high-inclination prograde orbits are most favorable and low-inclination retrograde orbits are least favorable (left). Furthermore, an impact while the comet is inbound is more difficult to mitigate than if the impact were while the comet is outbound (right). The latter phenomenon is explained by the comet's final approach to Earth: a comet approaching from within the Earth's orbit (outbound) approaches more rapidly and spends less time near the Earth than an otherwise identical comet approaching from beyond Earth's orbit (inbound). In all cases, the variation in effectiveness from orbital differences is, at most, comparable to the variation in $A_{1\,\rm km}$ between comets.[14]

Generally, deflection is most effective for orbits that place the comet near the laser for long durations over the deflection period since $\ddot{x}_{\rm NG}$ is an increasing function of $j \propto \Delta^{-2}$.

Figure 6 shows the variations in effectiveness for a $L_{\rm las} = 500\,$m, $P = 100\langle P\rangle$ laser deflecting an otherwise canonical comet beginning at $T - 1\,$yr over a range of plausible orbital parameters. For this case, high-inclination prograde orbits are most favorable and low-inclination retrograde orbits are least favorable. Furthermore, an impact while the comet is inbound is more difficult to mitigate than if the impact were while the comet is outbound. The latter phenomenon is explained by the comet's final approach to Earth: a comet approaching

from within the Earth's orbit (outbound) approaches more rapidly and spends less time near the Earth than an otherwise identical comet approaching from beyond Earth's orbit (inbound). In all cases, the variation in effectiveness from orbital differences is within a factor 2—comparable to the variation in $A_{1\,\mathrm{km}}$ between dynamically similar comets.[14]

Lasers with larger L_{las} starting at earlier t_0 experience increasingly less variation between comets of different orbits as deflection occurs over a spatial scale much larger than Earth's orbit with $j > j_0$ over a much longer distance. At such scale, the gravitational potential of the solar system is nearly isotropic about the laser (which, at large scale, is located near the center of the solar system) and deflection approaches the orbit-neutral limit. Conversely, small lasers are affected more strongly by the orbit of the comet, an effect than becomes important for ground-based lasers which may be useful for deflection at much smaller scales.

3.2 Ground Laser

Unlike for orbital arrays, $\langle P \rangle$ is not restricted by L_{las} for ground-based arrays where electric power is supplied externally. For a given P, $\langle P \rangle$ is only restricted by the requirement that the comet be within the laser's field of view Θ_{fov} and that weather conditions permit operation. Achieving the necessary diffraction-limited beam poses a serious challenge for very large $L_{\mathrm{las}} \implies$ tiny θ_{beam}. These constraints favor compact but high-powered arrays.

Ground-based lasers are directionally-biased by nature of their fixed field of view relative to Earth. A laser at latitude ϕ_{las} with field of view Θ_{fov} may only target comets in declinations $\phi_{\mathrm{las}} - \Theta_{\mathrm{fov}}/2 < \delta_{\mathrm{com}} < \phi_{\mathrm{las}} + \Theta_{\mathrm{fov}}/2$. A laser at a far northern latitude is completely ineffective against a comet approaching from near the south celestial pole as such a comet never rises sufficiently high in the sky to enter the laser's field of view.

Figure 7 compares the effectiveness of deflection of a set of modified canonical comets of various i by a $L_{\mathrm{las}} = 100\,\mathrm{m}$, $P = 10\,\mathrm{GW}$ array at $\kappa = 50\%$ for $\Theta_{\mathrm{fov}} = 90°$ and $\Theta_{\mathrm{fov}} = 60°$. The laser with the larger 90° field of view targets the comet longer than a laser with the smaller 60° field of view and thus produces a larger deflection Δ_{def} and is effective over a wider range of latitudes ϕ_{las}. Prograde orbits ($i < 90°$) are strongly favored over retrograde ($i > 90°$) due to prograde orbiting comets having slower relative velocity in the final approach. These

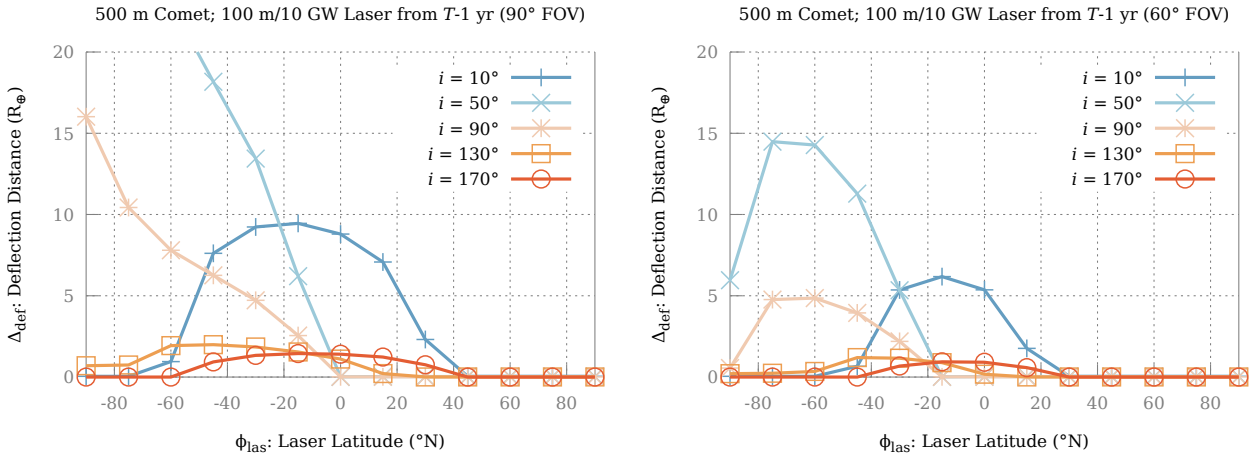

Figure 7. Under identical weather conditions ($\kappa = 50\%$), a ground-based laser is most effective when placed at a latitude ϕ_{las} similar to the declination of the target comet δ_{com}. A laser with a 90° field of view (left) is able to target the comet longer than a laser with a 60° field of view (right) and thus produces a larger deflection Δ_{def} and is effective over a wider range of latitudes. In addition, at $L_{\mathrm{las}} = 100\,\mathrm{m}$, prograde orbits ($i < 90°$) are strongly favored over retrograde ($i > 90°$) due to the prograde orbits' slower relative velocity. The simulations consider an Earth encounter at the comet's ascending node where the comet approaches from below the ecliptic, favoring deflection from the southern hemisphere for these cases. A descending node encounter would yield similar results, but mirrored to favor deflection from the northern hemisphere.

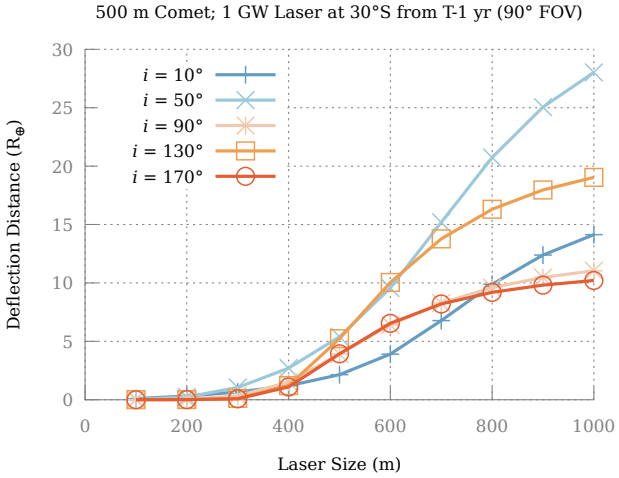

Figure 8. For a fixed $P = 1\,\mathrm{GW}$, deflection effectiveness rises rapidly with array size. A $L_{\mathrm{las}} = 500\,\mathrm{m}$ array at $P = 1\,\mathrm{GW}$ is of comparable effectiveness in deflecting a $2R_{\mathrm{com}} = 500\,\mathrm{m}$ comet as a smaller $L_{\mathrm{las}} = 100\,\mathrm{m}$ operating at a much higher $P = 10\,\mathrm{GW}$. Expanding the array to $L_{\mathrm{las}} = 1\,\mathrm{km}$ further increases deflection by $2-6\times$ to a very safe $\Delta_{\mathrm{def}} = 10\,\mathrm{R}_{\oplus}$ to $30\,\mathrm{R}_{\oplus}$ depending on orbit.

variations for the $L_{\mathrm{las}} = 100\,\mathrm{m}$ ground laser are far more significant than those of the $L_{\mathrm{las}} = 500\,\mathrm{m}$ orbital laser due to the spatial scale differences discussed in the previous section.

Lower P may be balanced by larger L_{las}. Figure 8 compares the deflection effectiveness by $P = 1\,\mathrm{GW}$ arrays over a range of L_{las}. A $L_{\mathrm{las}} = 500\,\mathrm{m}$ array at $P = 1\,\mathrm{GW}$ is of comparable effectiveness in deflecting a $2R_{\mathrm{com}} = 500\,\mathrm{m}$ comet as a smaller $L_{\mathrm{las}} = 100\,\mathrm{m}$ operating at a much higher $P = 10\,\mathrm{GW}$. A larger $L_{\mathrm{las}} = 1\,\mathrm{km}$ further increases the deflection by $2-5\times$ to a very safe $\Delta_{\mathrm{def}} = 10\,\mathrm{R}_{\oplus}$ to $30\,\mathrm{R}_{\oplus}$ depending on the comet's orbit.

Extremely large and powerful ground-based laser arrays of $L_{\mathrm{las}} = 1\,\mathrm{km}$ and $P = 100\,\mathrm{GW}$ have been proposed to enable near-relativistic spaceflight by radiation pressure on thin, reflective sails.[18] Such laser arrays, however, may only operate for a short fraction $\tau \ll 1$ of each day. Figure 9 compares deflection of comets of various sizes for $\tau = 100\,\mathrm{s/d}$ to $500\,\mathrm{s/d}$. An array at $\tau = 100\,\mathrm{s/d}$, installed at an appropriate site, can safely deflect a comet

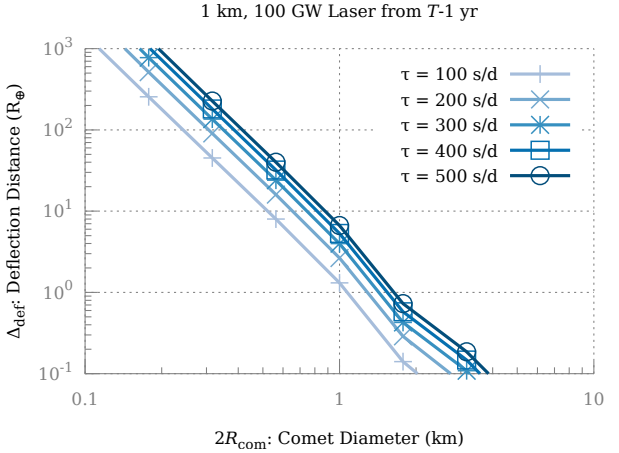

Figure 9. A large $L_{\mathrm{las}} = 1\,\mathrm{km}$ operating at $P = 100\,\mathrm{GW}$ for $\tau = 100\,\mathrm{s/d}$ over $1\,\mathrm{yr}$ is capable of deflecting a $2R_{\mathrm{com}} = 500\,\mathrm{m}$ by a comfortable $\Delta_{\mathrm{def}} \sim 10\,\mathrm{R}_{\oplus}$. Due to the short duration of laser activity, Δ_{def} is unaffected by laser location provided the comet enters the laser's field of view daily and remains for a duration $\geq \tau$.

as large as $2R_{\rm com} = 500\,{\rm m}$ by a comfortable $\Delta_{\rm def} \sim 10\,{\rm R}_\oplus$ over 1 yr. With $\tau = 500\,{\rm s/d}$, the same laser can deflect a $2R_{\rm com} = 1\,{\rm km}$ by nearly the same distance. A set of such lasers spanning both hemispheres will provide adequate defense against any realistic threat by an active comet for millennia to come.

4. CONCLUSIONS

Comets pose unique challenges left unanswered by most asteroid impact mitigation techniques. Their often near-parabolic orbits hinder discovery until, at best, a few years before impact. The expected uncertainties in trajectory for a newly-discovered object, particularly in A, introduce further delays to a response. The rapid timeline from discovery to impact coupled with often extreme delta-v requirements renders interception missions either unreliable or otherwise impractical with presently-known propulsion technologies.

This lack of attention stems in part from the rarity of comets relative to near-Earth asteroids. Comets of all groups are estimated to be responsible for less than 1% of all impact events in Earth's recent geological record though they may comprise the majority of large impactors of diameter $2R_{\rm com} \gtrsim 1\,{\rm km}$.[19] No comets of any size are confirmed to have impacted the Earth in the historical past nor is one expected to impact anytime in the foreseeable future. Hence, the threat of comets is of lower urgency than that of smaller but more common asteroids from which impacts have been observed in recent history.

Even so, given their unpredictable timing and the planet-scale disaster that likely follows impact, comet deflection remains an important consideration in planetary defense strategy. Further attention should be placed on the possibility and effects of comet disintegration in deflection—an important possibility neglected here—as well as other unintended consequences including dust generation which may prove fatal to insufficiently shielded satellites in Earth orbit.[20] Attention must naturally also be directed towards the engineering challenges of large scale laser arrays. Unless a strategy is prepared and a system is developed and primed before discovery, impact mitigation will be improbable. However, given adequate preparation, these preliminary simulations suggest that use of large, high-powered laser arrays of $L_{\rm las} \sim 0.1 - 1\,{\rm km}$—either in Earth orbit or, with advancements in adaptive optics technology, on the ground—may prove to be a viable strategy to mitigate comet impacts.

ACKNOWLEDGMENTS

We gratefully acknowledge funding from the NASA California Space Grant NNX10AT93H and from NASA NIAC NNX15AL91G and NNX16AL32G as well as a generous gift from the Emmett and Gladys W. Fund in support of this research. GNU Parallel was used in generating the presented simulation results.[21]

REFERENCES

1. C. R. McInnes, "Deflection of near-earth asteroids by kinetic energy impacts from retrograde orbits," *P&SS* **52**(7), p. 587, 2004.
2. J. D. Koenig and C. F. Chyba, "Impact deflection of potentially hazardous asteroids using current launch vehicles," *Science and Global Security* **15**(1), pp. 57–83, 2007.
3. R. Walker, D. Izzo, C. de Negueruela, L. Summerer, M. Ayre, and M. Vasile, "Concepts for near-earth asteroid deflection using spacecraft with advanced nuclear and solar electric propulsion systems," *JBIS* **58**(7–8), pp. 268–278, 2005.
4. R. Schweickart, C. Chapman, D. Durda, and P. Hut, "Threat mitigation: the gravity tractor." arXiv:physics/0608157, 2006.
5. D. C. Hyland, H. A. Altwaijry, S. Ge, R. Margulieux, J. Doyle, J. Sandberg, B. Young, X. Bai, J. Lopez, and N. Satak, "A permanently-acting nea damage mitigation technique via the yarkovsky effect," *CosRe* **48**(5), pp. 430–436, 2010.
6. M. Vasile and C. A. Maddock, "On the deflection of asteroids with mirrors," *CeMDA* **107**(1), pp. 265–284, 2010.
7. P. J. Francis, "The demographics of long-period comets," *ApJ* **635**(2), p. 1348, 2005.
8. P. Lubin, G. B. Hughes, J. Bible, J. Bublitz, J. Arriola, C. Motta, J. Suen, I. Johansson, J. Riley, N. Sarvian, D. Clayton-Warwick, J. Wu, A. Milich, M. Oleson, M. Pryor, P. Krogen, M. Kangas, and H. O'Neill, "Toward directed energy planetary defense," *OptEn* **53**, p. 025103, Feb. 2014.

9. Q. Zhang, K. J. Walsh, C. Melis, G. B. Hughes, and P. M. Lubin, "Orbital simulations on deflecting near-earth objects by directed energy," *PASP* **128**(962), p. 045001, 2016.
10. W. Folkner, J. Williams, and D. Boggs, "The planetary and lunar ephemeris de 421," Memorandum IOM 343R-08-003, Jet Propulsion Laboratory, 2008.
11. W. Kahan and R.-C. Li, "Composition constants for raising the orders of unconventional schemes for ordinary differential equations," *MaCom* **66**(219), pp. 1089–1099, 1997.
12. B. G. Marsden, Z. Sekanina, and D. Yeomans, "Comets and nongravitational forces. v," *AJ* **78**, p. 211, 1973.
13. A. Delsemme and D. Miller, "Physico-chemical phenomena in comets–iii: The continuum of comet burnham (1960 ii)," *P&SS* **19**(10), pp. 1229–1257, 1971.
14. D. K. Yeomans, P. W. Chodas, G. Sitarski, S. Szutowicz, and M. Królikowska, "Cometary orbit determination and nongravitational forces," in *Comets II*, G. W. Kronk, ed., pp. 137–151, Univ. of Arizona Press, 2004.
15. G. Kopp, G. Lawrence, and G. Rottman, "The total irradiance monitor (tim): science results," in *The Solar Radiation and Climate Experiment (SORCE)*, pp. 129–139, Springer, 2005.
16. D. Farnocchia, S. R. Chesley, P. W. Chodas, P. Tricarico, M. S. P. Kelley, and T. L. Farnham, "Trajectory analysis for the nucleus and dust of comet c/2013 a1 (siding spring)," *ApJ* **790**(2), p. 114, 2014.
17. E. M. Shoemaker, R. F. Wolfe, and C. S. Shoemaker, "Asteroid and comet flux in the neighborhood of earth," *Geological Society of America Special Papers* **247**, pp. 155–170, 1990.
18. P. Lubin, "A roadmap to interstellar flight," *ArXiv e-prints* , 2016.
19. D. K. Yeomans and A. B. Chamberlin, "Comparing the earth impact flux from comets and near-earth asteroids," *AcAau* **90**, pp. 3–5, Sept. 2013.
20. M. Beech, P. Brown, and J. Jones, "The potential danger to space platforms from meteor storm activity," *QJRAS* **36**, p. 127, 1995.
21. O. Tange, "Gnu parallel - the command-line power tool," *;login: The USENIX Magazine* **36**, pp. 42–47, Feb 2011.